

1           **Impact of meteorological conditions on BVOC emission rate from Eastern**  
2                           **Mediterranean vegetation under drought**

3  
4 Qian Li<sup>1,2</sup>, Gil ~~Lerner~~<sup>1</sup>Lerner<sup>2</sup>, Einat ~~Bar~~<sup>2</sup>Bar<sup>3</sup>, Efraim ~~Lewinsohn~~<sup>2</sup>Lewinsohn<sup>3</sup>, Eran  
5 ~~Tas~~<sup>1</sup>Tas<sup>2\*</sup>

6 <sup>1</sup> School of Ecology, Hainan University, No 58, Renmin Avenue, Haikou, Hainan province,  
7 China ~~Institute of Environmental Sciences, The Robert H. Smith Faculty of Agriculture, Food and~~  
8 ~~Environment, The Hebrew University of Jerusalem, P.O. Box 12, Rehovot 7610001, Israel~~

9 <sup>2</sup> Institute of Environmental Sciences, The Robert H. Smith Faculty of Agriculture, Food and  
10 Environment, The Hebrew University of Jerusalem, P.O. Box 12, Rehovot 7610001, Israel

11 ~~Department of Vegetable Research, Agricultural Research Organization – Neve Ya'ar Center,~~  
12 ~~Israel~~

13 <sup>3</sup> Department of Vegetable Research, Agricultural Research Organization – Neve Ya'ar Center,  
14 Israel

15  
16  
17  
18  
19 \* Correspondence to:

20 Eran Tas, Institute of Environmental Sciences, The Robert H. Smith Faculty of Agriculture, Food  
21 and Environment, The Hebrew University of Jerusalem, P.O. Box 12, Rehovot 7610001, Israel  
22 [eran.tas@mail.huji.ac.il](mailto:eran.tas@mail.huji.ac.il)

23 **Abstract**

24 A comprehensive characterization of drought's impact on biogenic volatile organic  
25 compounds (BVOC) emissions is essential for understanding atmospheric chemistry under  
26 global climate change, with implications for both air quality and climate model simulation.  
27 Currently, the effects of drought on BVOC emissions are not well characterized. Our study  
28 aims to test: i) whether instantaneous changes in meteorological conditions can serve as a  
29 better proxy for drought-related changes in BVOC emission compared to the absolute  
30 values of the meteorological parameters, as indicated in a companion article based on  
31 BVOC mixing-ratio measurements; ii) the impact of a plant under drought stress receiving  
32 a small amount of precipitation on BVOC emission rate, and on the manner in which the  
33 emission rate is influenced by meteorological parameters. To address these objectives, we  
34 conducted our study during the warm and dry summer conditions of the Eastern  
35 Mediterranean region, focusing on the impact of drought on BVOC emissions from natural  
36 vegetation. Specifically, we conducted branch-enclosure sampling measurements in Ramat  
37 Hanadiv Nature Park, both under natural drought and after irrigation (equivalent to 5.5–7  
38 mm precipitation), for six selected branches of *Phillyrea latifolia*, the highest BVOC  
39 emitter in this park, in September–October 2020. The samplings were followed by gas  
40 chromatography-mass spectrometry analysis for BVOCs identification and flux  
41 quantification. The results corroborate the finding that instantaneous changes in  
42 meteorological parameters, particularly relative humidity (RH), offer the most accurate  
43 proxy for BVOC emission rates under drought, compared to the absolute values of either  
44 temperature (T) or RH. However, after irrigation, the correlation of the detected BVOC  
45 emission rate with the instantaneous changes in RH became significantly more moderate,

46 or even reversed. Our findings highlight that under drought, the instantaneous changes in  
47 RH, and to a lesser extent in T, are the best proxy for the emission rate of monoterpenes  
48 (MTs) and sesquiterpenes (SQTs), whereas under moderate drought conditions, T or RH  
49 serves as the best proxy for MT and SQT emission rate, respectively. In addition, the  
50 detected emission rates of MTs and SQTs increased by 150% and 545%, respectively, after  
51 a small amount of irrigation.

52

## 53 **1 Introduction**

54 Biogenic volatile organic compounds (BVOCs) are released by plants and other organisms  
55 to the atmosphere. They play a critical role in both climate change and photochemical air  
56 pollution (Cai et al., 2021; Calfapietra et al., 2013; Curci et al., 2009; Guenther, 2013;  
57 Kesselmeier and Staudt, 1999; Peñuelas et al., 2009). BVOCs are thought to be emitted by  
58 plants as a defense mechanism against biotic and abiotic stresses, such as herbivory and  
59 high temperatures (Berg et al., 2013; Blande et al., 2007; Brilli et al., 2009; Peñuelas and  
60 Munné-Bosch, 2005). BVOCs may also be involved in plant–plant and plant–animal  
61 communication, allowing plants to signal to other organisms about their response to  
62 environmental conditions (Baldwin et al., 2006; Filella et al., 2013; Niinemets and Monson,  
63 2013).

64 The emission rate and composition of BVOCs can vary widely depending on  
65 various factors, such as meteorological conditions, rate of synthesis, and physicochemical  
66 properties (Niinemets and Monson, 2013). Climate change is expected to significantly  
67 impact BVOC emission rate and composition. As temperature rises, the emission rate of  
68 most BVOCs increases in an Arrhenius-type manner (Goldstein et al., 2004; Greenberg et

69 al., 2012; Guenther et al., 1995; Monson et al., 1992; Niinemets et al., 2004; Tingey et al.,  
70 1990). On the other hand, drought can have a more complex effect on the emission and  
71 composition of BVOCs. Depending on the type of vegetation, the level of drought stress,  
72 and additional ambient conditions, the emission of BVOCs can be partially or completely  
73 suppressed (Fortunati et al., 2008; Holopainen and Gershenson, 2010; Llusia et al., 2016;  
74 Peñuelas and Staudt, 2010; Schade et al., 1999), or enhanced in a way that has not yet been  
75 characterized (Fitzky et al., 2023; Geron et al., 2016; Potosnak et al., 2014).

76         The effect of drought on isoprene emission has been extensively studied, and it was  
77 discovered to be postponed relative to, and/or less significant than the effect on  
78 photosynthetic rate (Asensio et al., 2007; Brillì et al., 2007; Fortunati et al., 2008; Pegoraro  
79 et al., 2006; Ryan et al., 2014). However, whereas under moderate drought stress, isoprene  
80 emission may only slightly decrease or increase, it was shown to decrease considerably  
81 under severe or prolonged drought stress (Fortunati et al., 2008; Han et al., 2022; Jiang et  
82 al., 2018). The impact of drought on the emission of other BVOCs, such as monoterpenes  
83 (MTs) and sesquiterpenes (SQTs), has been less studied.

84         The Eastern Mediterranean has a unique climate characterized by a hot and dry  
85 summer, making it an ideal location to study the impact of drought on BVOC emissions.  
86 The semiarid and arid regions are particularly vulnerable to climate change, and climate  
87 simulations predict that the Eastern Mediterranean region will experience more frequent  
88 and severe droughts in the future (Giorgi and Lionello, 2008; Lionello, 2012). Research  
89 conducted in Israel has investigated the impact of drought on BVOC emissions from a  
90 range of local plant species. For example, Llusia et al. (2016) examined the effect of  
91 drought on terpene emission from Yatir Forest, a pine forest in the northern Negev. They

92 found that some of the MT and SQT emissions increased under moderate drought  
93 conditions but strongly decreased under severe drought conditions. Another measurement  
94 by Li et al. (2024), performed in late autumn 2016 in Shibli Forest in northern Israel, found  
95 that under severe drought stress, BVOC emissions respond more significantly to the  
96 instantaneous changes in meteorological parameters (especially relative humidity [RH])  
97 than to the meteorological parameters themselves. These studies suggest that the impact of  
98 drought on BVOC emissions is not well-characterized and varies in a complex manner,  
99 depending on plant species, BVOC type, and meteorological parameters, such as  
100 temperature (T) and RH, as well as the level of drought stress. Hence, more research is  
101 needed to better characterize the effect of drought on BVOC emission rates and  
102 composition, which can in turn improve air quality and climate modeling.

103 In this study, we use the severe drought conditions during the autumn in the Eastern  
104 Mediterranean to study the effect of drought on the emission of BVOCs from natural  
105 vegetation. The main specific objectives of this study were to: i) identify whether  
106 instantaneous changes in meteorological parameters can serve as a better proxy for BVOC  
107 emission rates under drought than their absolute values, and ii) determine the extent to  
108 which small precipitation amounts, under drought conditions, can impact BVOC emission  
109 rates and the manner in which the emission rate is influenced by meteorological parameters.  
110

## 111 **2 Methods**

112 We used an enclosure-based measurement system to quantify BVOC emissions, allowing  
113 for direct measurement of BVOC fluxes at the branch level. The measurements were  
114 performed in autumn under the prolonged drought stress conditions typical to this region.

115 BVOC measurements in the Eastern Mediterranean are rare, and to the best of our  
116 knowledge, our study is the first to apply direct measurements of BVOC flux from specific  
117 branches of natural vegetation in this region. Plants were sampled before and after the  
118 application of a small amount of irrigation to study the response of BVOC emissions, under  
119 exposure to natural drought conditions, to a small amount of precipitation. This was  
120 followed by gas chromatography–mass spectrometry (GC–MS) to identify and quantify  
121 the emitted BVOCs. Closed chambers are often used for measurements of BVOCs at the  
122 branch level (Duhl et al., 2008). Compared to open-system methods, the enclosure-based  
123 system (including a glass cuvette or Tedlar bag) can focus on specific vegetation in a more  
124 controlled manner. To investigate the effects of drought on BVOC emission rates and  
125 composition, we performed two sets of measurements – before and after irrigation – for  
126 comparison. To study the effect of meteorological conditions on BVOC flux, we monitored  
127 meteorological parameters inside the bag and at a meteorological station that was 300–600  
128 m from the branches.

129

### 130 *2.1 Sampling site and studied species*

131 The on-site branch measurements were conducted at Ramat Hanadiv Nature Park (32°  
132 33' 19.87" N, 34° 56' 50.23" E), 3.6 km from the Eastern Mediterranean seashore and  
133 exposed to a typical Eastern Mediterranean climate, with annual precipitation of 640 mm  
134 (averaged over the last 5 years, and occurring mainly between November and March). The  
135 vegetation at the site is dominated by mixed Mediterranean shrubbery. More details about  
136 the site and vegetation can be found in Li et al. (2018) and Dayan et al. (2020). The  
137 measurements were conducted at the end of summer/beginning of autumn under drought

138 conditions. No precipitation was recorded for 108 days between 24 May 2020 and the  
139 beginning of the study on 9 Sep 2020.

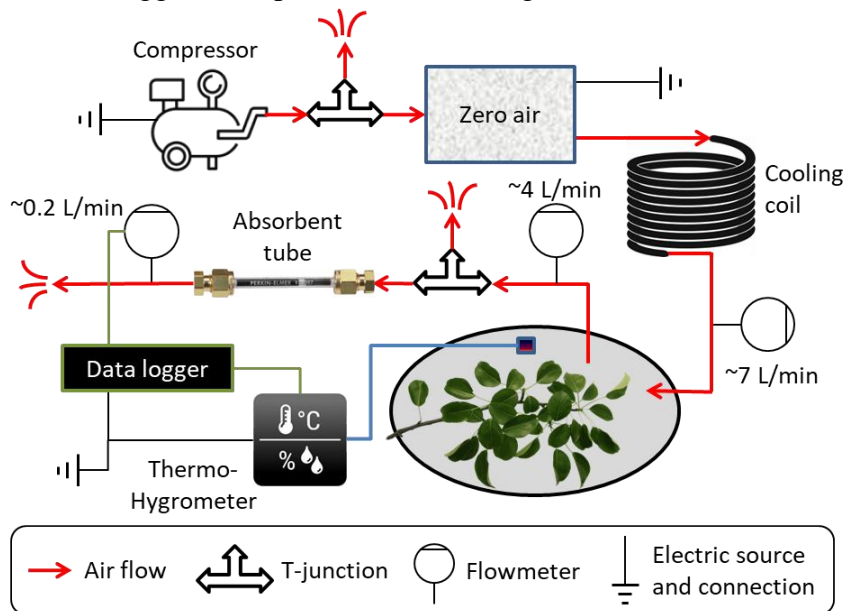
140 *Phillyrea latifolia* (broad-leaved phillyrea), identified as the greatest BVOC-  
141 contributing plant species in the Ramat Hanadiv natural park, was sampled. The species is  
142 native to the Mediterranean Basin and belongs to the family Oleaceae. In Ramat Hanadiv,  
143 it accounts for 7.5% of all vegetation, but up to ~35% of all BVOC emissions, according  
144 to the Model of Emissions of Gases and Aerosols from Nature (MEGAN v2.1; Dayan et  
145 al., 2020; Guenther et al., 2012; Li et al., 2018). The selected plants were mature and did  
146 not show any visible signs of senescence. Sampled branches were shaded, to eliminate the  
147 effect of non-natural high temperature in the enclosure system, and measurements were  
148 performed at 1.5 to 2 m aboveground.

149

## 150 ***2.2 Branch-enclosure sampling system and setup***

151 Figure 1 presents a self-made branch-sampling system was used for this study. All tubes  
152 and connections are Teflon, while valves and flowmeters are stainless steel. A compressor  
153 provides a controllable rate of ambient air flow through an adjustable T-junction valve (to  
154 adjust the flow rate) to a zero-air device (Model 1150 dual reactor, Thermo Fisher  
155 Scientific, Waltham, MA, USA), which includes a catalytic converter heated to ~350 °C to  
156 oxidize carbon monoxide (CO) and hydrocarbons (HC) to carbon dioxide (CO<sub>2</sub>-) and water  
157 (H<sub>2</sub>O). From the zero-air device, the air flows through a copper coil to cool it down, and  
158 then through a mass flowmeter into a Tedlar bag (CEL Scientific Corporation, Cerritos,  
159 CA, USA), at a flow rate of about 7 L min<sup>-1</sup> (monitored by flowmeter A), a high enough  
160 inflow to produce slight overpressure inside the bag. The inert and light-transparent 10 L

161 Tedlar bag is tied tightly around a tree branch, along with an EL-MOTE-TH temperature  
 162 and RH sensor (Lascar Electronics, Whiteparish, Wiltshire, UK). The outlet airflow ( $\sim 4$  L  
 163  $\text{min}^{-1}$  monitored by flowmeter B) is directed to the C2-CAXX-5032 hydrophobic inert-  
 164 coated stainless-steel adsorbent tube (CSLR, Markes International, Llantrisant, UK)  
 165 precoated-filled with a mixture of Tenax TA and Carbograph as adsorbent, at a rate of  $\sim 0.2$   
 166 L  $\text{min}^{-1}$  (monitored by flowmeter C), regulated by the T-junction valve downstream of  
 167 flowmeter B. The flow rate through the adsorbent tube, as well as T and RH were recorded  
 168 with a CR1000 data logger (Campbell Scientific, Logan, UT, USA).



169 **Figure 1.** Schematic of the branch-enclosure sampling system. VOCs are removed from the ambient air  
 170 before entering a transparent Tedlar bag and an adsorbent tube to monitor BVOC emissions from the enclosed  
 171 branch, using a flow-controlled system (see Sect. 2.2).

172

### 173 *2.3 Analytical quantification of the sampled BVOCs*

174 A Centri™ (Markes International) preconcentration system was used to desorb the tubes  
 175 into the cold trap (graphitized carbon trap; used for sampling VOCs of C4/5 to C30/32)  
 176 under the following conditions: desorption for 5 min at 280 °C with a trap flow of 30 mL



177 min<sup>-1</sup>. Desorption of trap was at a rate of 20 °C s<sup>-1</sup> to 300 °C into an Agilent GC–MS  
178 (7890A/5975C) system (Santa Clara, CA, USA) equipped with a Stabilwax column  
179 (Restek, 30 m, 0.25 mm ID capillary column; polyethylene glycol, 0.25 µm film thickness).  
180 The general run parameters were as follows: injector, 230 °C; column oven, initial  
181 temperature of 45 °C for 5 min, followed by a ramp of 5 °C min<sup>-1</sup> to 120 °C, 20 °C min<sup>-1</sup>  
182 to 240 °C final, and 5-min hold with a total run time of 31.5 min; carrier gas, He 32 psi;  
183 mass spectrometer ionization energy, 70 eV; m/z, 41 to 300; scan time, 5.4 s. The  
184 chromatograms were analyzed using MassHunter Quant Analysis (B.10.00, Agilent  
185 Technologies, Santa Clara, CA, USA) software. Compounds were identified by comparing  
186 their relative retention indices and mass spectra with those of authentic standards or those  
187 found in the literature, supplemented with W10N14 and 2205 GC–MS libraries.

188 We chose to analyze the most abundant BVOC species: *cis*-β-ocimene (E, Z) (MT),  
189 and β-caryophyllene, α-humulene, α-farnesene, germacrene-D (SQTs). For calibration,  
190 analytical-grade standard solutions (7–12 concentrations) were prepared, ranging in  
191 concentrations from 0.25 to 1000 ng mL<sup>-1</sup> by diluting known masses of pure chemicals  
192 with methanol. The calibration analytes were injected using a GC syringe onto clean  
193 sorbent tubes connected to a calibration solution-loading rig (Markes International) at a  
194 nitrogen flow of 80 mL min<sup>-1</sup> for 5 minutes. The standards for the BVOC species were *cis*-  
195 β-ocimene (E, Z) (W353977, Sigma-Aldrich) (MT), and β-caryophyllene (22075-1ML-F,  
196 Sigma-Aldrich), α-humulene (PHL83351, Sigma-Aldrich), α-farnesene (Biosynth®  
197 Carbosynth Ltd., UK), germacrene-D (Toronto Research Chemicals, Canada) (SQTs),  
198 according to the most abundant species (see Sect. 2.4). where †The sampled solution base  
199 was mixed with 5 µL of each compound in the solvent. All standard-loaded tubes were

200 prepared in triplicate and results were averaged. The loaded tubes were analyzed under the  
201 same conditions used for the other samples. Standard curves of peak area counts vs. VOC  
202 mass ( $\mu\text{g}$ ) were fitted using linear regression analyses; both yielded high regression  
203 coefficients ( $r^2 \geq 0.99$  in most cases). More details on the calibration are provided in Sect.

204 S1. As for the minor MTs and SQTs, the calibration curve of *cis*- $\beta$ -ocimene (E, Z) and  
205 the averaged calibration curve of the four most abundant SQTs were used for a rough  
206 estimation of their emission rates.

207

## 208 ***2.4 Experimental setup***

### 209 ***2.4.1 Branch sampling, meteorological parameter measurements and flux evaluation***

210 The field measurements were performed from late summer to early autumn – 9 Sep to 27  
211 Oct 2020. Samplings were conducted on six selected *Phillyrea latifolia* branches on  
212 different bushes. Each branch was measured over two sequential days: 8–9 Sep, 14–15 Sep,  
213 22–23 Sep, 12–13 Oct, 19–20 Oct, and 26–27 Oct. The bushes were at least 20 m apart, to  
214 enable selective irrigation for individual shrubs. Meteorological parameters were measured  
215 at a distance of 300–600 m from the branch measurements. These parameters included T  
216 and RH, measured using a Campbell HC2S3 probe; net radiation, measured with a CNR4  
217 Kipp & Zonen net radiometer; and wind speed and direction, recorded by a 05103 R.M.  
218 Young sensor. Eight 30-min samplings were performed per measurement day. In addition,  
219 two reference samplings were performed with full equipment setup, but no branch inside  
220 the bag. These reference samplings were performed before and after the eight  
221 measurements. On each measurement day, Prior after to completing the first reference  
222 sampling for reference, the system and branches were given at least 60 minutes to adapt to

223 the different conditions after placing the branch into the setup of the bag and setting up the  
224 equipment. At the end of the first measurement day, the sampled branch was removed from  
225 the bag and returned after the reference sampling on the second day. Following the ~~10<sup>th</sup>~~ 9<sup>th</sup>  
226 sampling on the second measurement day of each 2two-sequential-day period, the sampled  
227 branch was cut and sent to the laboratory for leaf analysis. Leaf ~~net dry~~ wet weight and area  
228 were evaluated within 24 h after cutting the branch. All leaves were scanned, and a digital  
229 color-based image-processing method was used to identify the total (RGB values: 40–200,  
230 50–200, 30–200) and healthy (RGB values: 40–110, 50–105, 30–80) leaf areas. The leaves  
231 were then dried for 72 h at 60 °C, and their net dry weight was recorded.

232 The sampling tubes were kept in a cooler with a temperature below 5 °C after the  
233 measurement, and analyzed within 5 days of sampling by GC–MS (see Sect. 2.3). Of the  
234 identified species, ~~the one~~ MT and four SQT compounds ~~with the highest sampled mass~~  
235 (*cis*-β-ocimene, β-caryophyllene, α-humulene, α-farnesene, and germacrene D) with the  
236 highest sampled mass for a~~each of the branches~~ were chosen for quantification by GC–  
237 MS (see Sect. 2.3).

238 The emission rate of BVOCs per leaf area,  $E_A$  (ng cm<sup>-2</sup> h<sup>-1</sup>), for a branch was  
239 evaluated by the following formula:

$$240 \quad E_A = \left( m \frac{F_{in-B}}{F_{out-T}} \right) / (A \cdot t) \quad (1)$$

241 where  $m$  (ng) is the evaluated mass of any BVOC compound inside the tube,  $F_{in-B}$  (L min<sup>-1</sup>)  
242 and  $F_{out-T}$  (mL min<sup>-1</sup>) are the flow rate pumped into the bag and the flow rate through  
243 the adsorbent tube, respectively,  $A$  (cm<sup>2</sup>) is the total leaf area of the branch, and  $t$  (h) is the  
244 sampling time.

245 The emission rate of BVOCs per biomass,  $E_M$  (ng g<sup>-2</sup> h<sup>-1</sup>), was evaluated by:

246 
$$E_M = \left( m \frac{F_{in-B}}{F_{out-T}} \right) / (M \cdot t) \quad (2)$$

247 where M (g) is the leaf biomass of the branch.

248

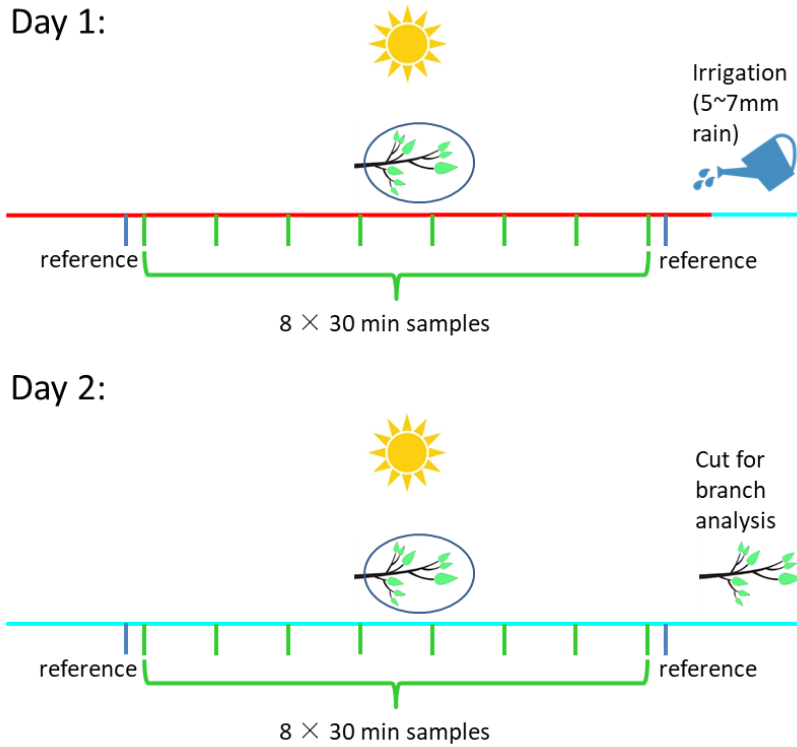
249 **2.4.2 Irrigation and soil-water content quantification**

250 Manual irrigation was applied at the end of the first measurement day of each 2-sequential-  
251 day measurement period (see Fig. 2). The irrigation amounts were 50–70 L within a radius  
252 of 1–2 m from the stem of the plants used for sampling (equivalent to 5.5–7 mm rain). This  
253 irrigation served to identify the potential effect of a small precipitation event during a  
254 drought period on BVOC emission rate and composition.

255 ~~Ten soil samples were collected at solar noon time within 2 m from the sampled~~  
256 ~~plant on every experimental day. To evaluate the soil water content, soil samples were~~  
257 ~~weighed on the day of collection, and weighed again after drying them in an oven at 105 °C~~  
258 ~~for 24 h. The following formula was used to calculate the soil water content:~~

259 
$$w = \frac{M_{tot} - M_{dry}}{M_{dry}} \times 100\% \quad (3)$$

260 ~~where w (g/g) is the soil gravimetric water content and  $M_{tot}$  (g) and  $M_{dry}$  (g) are the total~~  
261 ~~and dried soil mass, respectively.~~



262 **Figure 2.** Schematic of the experimental design. Day 1 and Day 2 represent, respectively, the first and  
 263 second day of each two-sequential-day sampling period for a specific branch. Green and blue bars represent  
 264 sampling measurements and reference measurements, respectively. The red and cyan lines mark sampling  
 265 prior to manual irrigation on Day 1 and after manual irrigation, on Day 2, respectively.

266 Ten soil samples were collected at solar noon time within 2 m from the sampled  
267 plant on every experimental day. To evaluate the soil-water content, soil samples were  
268 weighed on the day of collection, and weighed again after drying them in an oven at 105 °C  
269 for 24 h. The following formula was used to calculate the soil-water content:

270 
$$w = \frac{M_{tot} - M_{dry}}{M_{dry}} \times 100\% \quad (3)$$

271 where w (g/g) is the soil gravimetric water content and  $M_{tot}$  (g) and  $M_{dry}$  (g) are the total  
272 and dried soil mass, respectively.

273

274

275

### 276 **2.4.3 Correlation between BVOC emission rate and temporal changes in RH and T**

277 To test the effect of instantaneous changes in RH and T on the emission rate of the sampled  
278 BVOCs, we studied the correlation between the temporal changes in both ambient air RH  
279 and T with the BVOC emission rate during the sampling. BVOC sampling length was 30  
280 min, with a gap of 1 h between each sampling. To account for instantaneous changes in  
281 RH and T we introduce  $\delta_{RH}$  and  $\delta_T$ , respectively.  $\delta_{RH}$  is defined as follows:

$$282 \quad \delta_{RH} = \sum_{i=1}^n \left( \frac{RH_{i+1}}{RH_i} - 1 \right) \quad (4)$$

283 where  $i$  is the 10 min time step; according to the available measurement frequency which  
284 is the highest measurement frequency available, and  $n$  is the number of time steps.

285  $\delta_T$  is defined in the same manner as follows:

$$286 \quad \delta_T = \sum_{i=1}^n \left( \frac{T_{i+1}}{T_i} - 1 \right) \quad (5)$$

287 The correlations between  $\delta_{RH}$ ,  $\delta_T$  and the BVOC fluxes for all samples were tested  
288 for different values of  $n$ . In a preliminary test, it was found that the highest average  
289 correlations of  $\delta_{RH}$  and  $\delta_T$  with BVOC emission rate were obtained when  $n = 9$ .  
290 Accordingly, the calculation duration of  $\delta_{RH}$  and  $\delta_T$  began 60 min before each 30 min  
291 BVOC emission rate sampling. This finding is consistent with a similar analysis conducted  
292 by Li et al. (2024). Similarly, the correlation between  $\delta_{RH}$  and  $\delta_T$  and BVOC emission rate  
293 in that study applied  $\delta_{RH}$  and  $\delta_T$  which were calculated for 90 min cycles, while the  
294 beginning of each cycle was 60 min prior to the beginning of each compatible 30 min  
295 BVOC sampling.

296

### 297 **2.4.4 Afternoon emission trend (AET) analysis**

298 Under drought conditions, the increased stomatal resistance can largely reduce the BVOC  
299 emission rate (see Sect. 1). Accordingly, it was found that the BVOC mixing ratio tends to  
300 reach a minimum around noontime when RH tends to reach its daily minimum and stomatal  
301 conductance is limited (Nobel, 1999), and then gradually increase in the afternoon (Li et  
302 al., 2024). Our observations indicated a clear increase in BVOC emission rates during the  
303 afternoon for the days before the irrigation. On those days, no clear decrease in BVOC  
304 emission was observed before noon; instead, the BVOCs generally exhibited lower  
305 emission rates. Here we introduce a method for quantifying the trend of emission rate right  
306 after the mid-day minimum, which applies the afternoon emission trend (AET) index:

$$307 \quad \text{AET} = \sum_{i=1}^n \left( \frac{E_{i+1}}{E_i} - 1 \right) \quad (6)$$

308 where  $E_i$  is the emission rate of the  $i$ <sup>th</sup> sample, while  $i = 1$  indicates the ~~daily~~ minimum  
309 value around noontime, between 12:00–14:00 h. Hence, the AET indicates the trend and  
310 magnitude of the emission in the afternoon of any measurement day.



311

312

### 313 3 Results and discussion

#### 314 3.1 Analysis of branch leaves

315 Figure 3 shows the total leaf area (cm<sup>2</sup>), green leaf area (cm<sup>2</sup>), leaf water content, and soil  
316 moisture before and after irrigation of each sampling branch. Leaf green area ranged

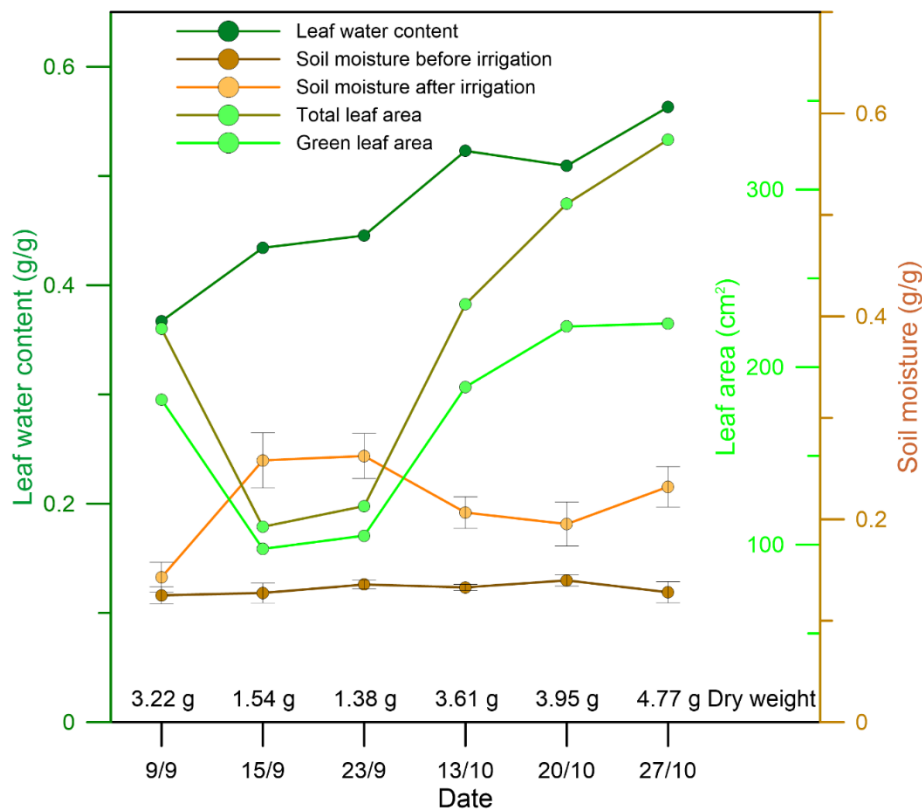
317 ~~between~~ from 68% to 89% of the total leaf area. Soil moisture ~~was around~~ ranged

318 ~~between~~ from 12.5% ~~and to~~ 14.0% before irrigation and ~~from~~ 14.3% ~~and to~~ 26.2%

319 after irrigation. Interestingly, the leaf water content after irrigation increased gradually

320 during the experimental period, indicating that the capacity for water uptake from the soil

321 increases with drought prolongation.



322 **Figure 3.** Properties of the sampled branch leaves and soil moisture within a radius of 1 m from the stem of  
323 the sampling plant. Presented leaf property values are averages over all sampled branch leaves.

324

325

326 ***3.2 Emission rates of MTs and SQTs***

327 Whereas previous branch enclosure studies focused primarily on isoprene emissions  
328 (Genard-Zielinski et al., 2015; Genard-Zielinski et al., 2018; Saunier et al., 2017), our  
329 measurements did not detect large amounts of isoprene emissions from the selected  
330 *Phillyrea latifolia*, in line with previous studies showing that some plant types do not emit  
331 notable amounts of isoprene (Aydin et al., 2014; Bracho-Nunez et al., 2013). Our analysis  
332 focused on the MTs and SQTs detected in our observations, as described in the following  
333 section.

334

335

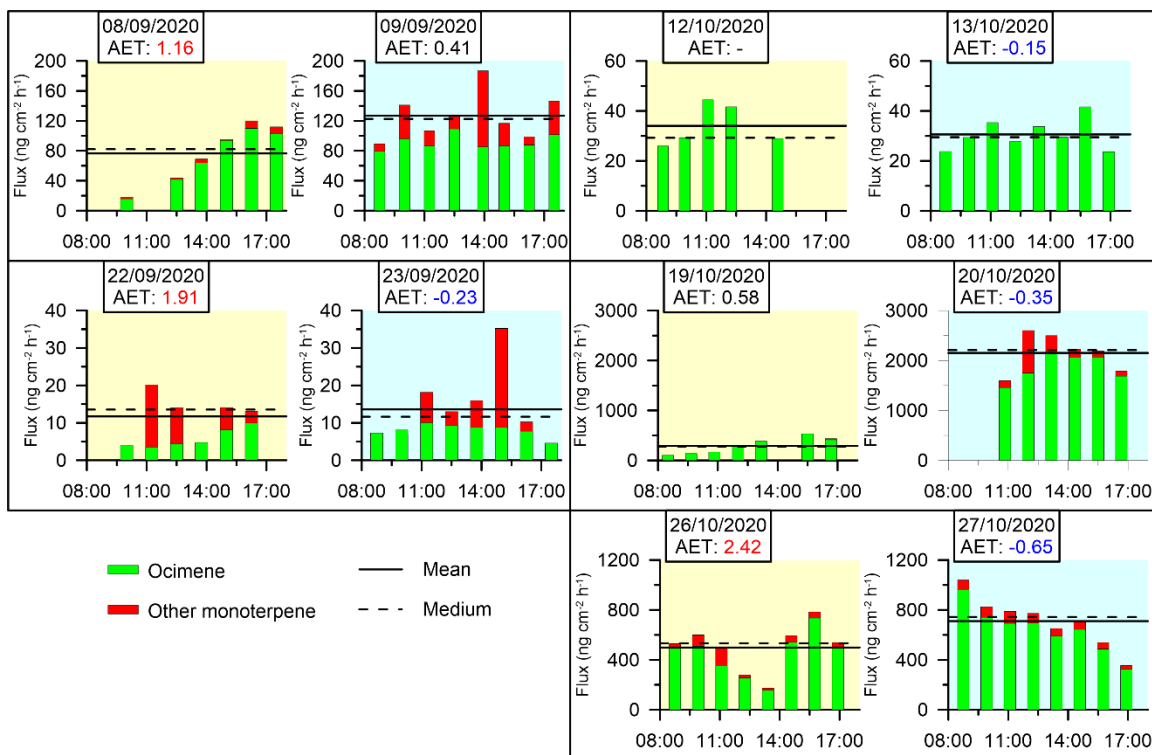
### 336 3.2.1 MTs

337 On all 10 sampling days for which MTs were identified, the 5 days prior to irrigation were  
338 under drought conditions (i.e., more than 100 days after the last precipitation event), and 5  
339 days were under irrigation conditions on the same branches (see Sect. 2.4.2). The branch  
340 which was sampled on Sep 14–15 did not show any detectable MT emission. The diurnal  
341 emission fluxes of MTs from the branches are shown in Fig. 4.

342 The daily average emission rate of MTs over all sampling days ranged from 11.7–  
343 2151.4 ng cm<sup>-2</sup> h<sup>-1</sup> (0.89–121.5 µg g<sup>-1</sup> h<sup>-1</sup>), with *cis*-β-ocimene being the most abundant for  
344 each of the sampling branches, averaging at 88% of all detected MTs. These MT  
345 emission rates are similar to previous branch enclosure studies, which were conducted  
346 predominantly between May and October under Western Mediterranean conditions, where  
347 they ranged from 0 to approximately 140 µg g<sup>-1</sup> h<sup>-1</sup> (Bracho-Nunez et al., 2013; Llusià and  
348 Peñuelas, 2000; Núñez et al., 2002; Owen et al., 1997; Owen and Hewitt, 2000; Staudt et  
349 al., 2001; Street et al., 1997). Less information is available on the emission rates of MTs in  
350 the Eastern Mediterranean. Aydin et al. (2014) used a branch enclosure system to detect  
351 emission rates ranging from 0.0047 to 14.2 µg g<sup>-1</sup> h<sup>-1</sup> in 14 different forested areas in  
352 Turkey. Seco et al. (2017) quantified MT emissions using eddy covariance method in pine  
353 forests in Israel, studying a semiarid site (Yatir) and a Mediterranean sub-humid site (Birya)  
354 in the spring. Emission fluxes were found to average at 40 ng cm<sup>-2</sup> h<sup>-1</sup> (Yatir) and 100 ng  
355 cm<sup>-2</sup> h<sup>-1</sup> (Birya), with peak values of 100 (Yatir) and 190 (Birya) ng cm<sup>-2</sup> h<sup>-1</sup>, while the  
356 daytime standardized MT emission capacities were similar across both sites.

357 In our study, MT emissions under drought conditions ranged from 11.7 ng cm<sup>-2</sup> h<sup>-1</sup>  
358 to 499.0 ng cm<sup>-2</sup> h<sup>-1</sup>, which is somewhat higher than other values reported in the Eastern  
359 Mediterranean. It is important to note that differences in emission rates between our study  
360 and the previously reported values in this region might be attributed to the different  
361 measurement methodologies employed. Following irrigation, the mean daily MT emission  
362 rates increased in four out of the five investigated branches, and ranged from 13.6 ng cm<sup>-2</sup>  
363 h<sup>-1</sup> to 2151.4 ng cm<sup>-2</sup> h<sup>-1</sup>. This reflects an average 150% increase for all sampling days in  
364 the range of emission rates following irrigation, indicating that even a small amount of  
365 water during a period of drought stress can significantly influence MT emissions. This  
366 effect may be related to the dramatic increase in stomatal conductance, due to the increase  
367 in water availability following irrigation (Medrano et al., 2002; Miyashita et al., 2005;  
368 Vilagrosa et al., 2003). It is was also observed that on some of the sampling days, the  
369 composition of MTs tends to become more diverse after irrigation compared to before  
370 irrigation, warranting further studiesyy.  
371 AET (Sect. 2.4.4) values specified in figures 4 and 5 reinforced the significant effect of  
372 small irrigation amounts on BVOC emission rates under drought, considering that on  
373 drought days, AETs were high and positive, whereas after irrigation, AETs became  
374 moderate or negative. This observation is consistent with previous studies showing that the  
375 emission of BVOCs can be affected by the vegetation's stomatal activity, which tends to  
376 be lower around noontime during drought stress (Li et al., 2023; Seco et al., 2017). Stomatal  
377 resistance is typically two orders of magnitude larger than cuticular resistance (Nobel, 1999)  
378 and therefore, the midday minimum and the following increase in MT emissions under  
379 drought conditions may be mostly due to stomatal resistance, which can limit the exchange

380 of gases between the plant and the atmosphere. In other words, the increased emission of  
 381 MTs after irrigation may be due to reopening of the stomata, which allows for the release  
 382 of VOCs.~~MTs after irrigation may be due to reopening of the stomata, which allows for~~  
 383 ~~the release of VOCs.~~



384 **Figure 4** Branches' diurnal MT emission fluxes. No MTs were detected for the branch sampled on 14–15  
 385 Sep. Yellow and blue shading indicate the days before and after irrigation, respectively (see Sect. 2.4.2).  
 386 Horizontal solid and dashed lines are daytime mean and median fluxes of MTs, respectively. AET values  
 387 (see Sect. 2.4.4) are marked in red and blue when they are larger than 1 or negative, respectively.

388

389

### 390 3.2.2 SQTs

391 Figure 5 shows the emission fluxes of SQTs for the branches under drought and irrigation  
 392 conditions. The four major-most abundant detected SQTs detected for all each of the  
 393 sampled branches were  $\beta$ -caryophyllene,  $\alpha$ -humulene, germacrene D, and  $\alpha$ -farnesene.

394 These compounds comprised 90% of all detected SQTs, from all the branches together.  
395 The daily average emission rate of SQTs ranged from 1.7–2595.7 ng cm<sup>-2</sup> h<sup>-1</sup> (0.11–146.6  
396 µg g<sup>-1</sup> h<sup>-1</sup>). In contrast to MTs, few studies provide branch enclosure measurements for  
397 SQTs. Notably, our study found significantly higher emission rates than previous research  
398 conducted between June and October under Eastern Mediterranean conditions, where rates  
399 ranged from 0.0011 to 0.63 µg g<sup>-1</sup> h<sup>-1</sup> (Aydin et al., 2014; Bracho-Nunez et al., 2013). The  
400 emission fluxes of the SQTs were overall comparable to those of the MTs, which is a  
401 notable finding, considering that SQT emission rates are frequently around a quarter of the  
402 MT flux (Saunders et al., 2003; Sindelarova et al., 2014). The finding of relatively high  
403 SQT emission rates appears to be in line with the findings of Li et al. (2023), who reported  
404 relatively high mixing ratios of SQTs (33.6 times higher than isoprene, and 18.9 times  
405 higher than MTs) under drought conditions in the same region.

406 Furthermore, we found that the increase in SQT emission flux following irrigation  
407 (by 545% on average) was more significant than that of the MTs (by 150% on average).  
408 This suggests that the response of SQT emissions to water availability is stronger than that  
409 of MTs, which could be related to the chemical properties and physiological functions of  
410 SQTs in plants. Bonn et al. (2019) found that a sharp increase in SQT emission occurs  
411 close to the wilting point to protect the plant against oxidative damage, as also supported  
412 by Caser et al. (2019). The latter found that drought can induce the SQT-synthesis close to  
413 the wilting point to protect the plant against oxidative damage, as also supported by Caser  
414 et al. (2019). The latter found that drought can induce the SQT synthesis mechanism. The  
415 strong increase in SQT emission after irrigation in our study further supports the notion  
416 that enhanced synthesis of SQTs occurs shortly after the release of drought stress. In

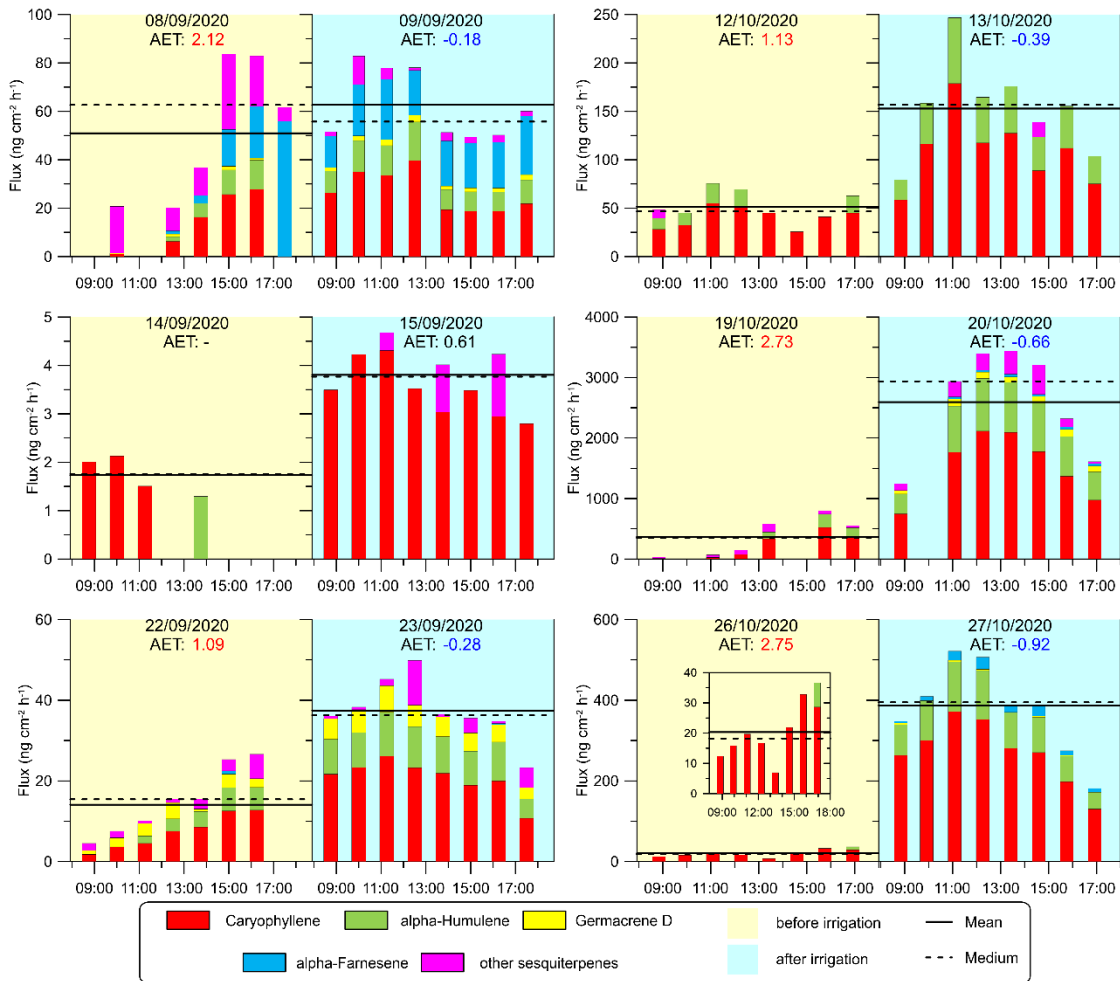
417 addition, the SQTs composition, like MTs composition, was observed to be more diverse  
418 after irrigation in most cases, warranting further study.

419 Interestingly, the high SQT emission rates found in this study are consistent with  
420 the findings of a previous study conducted in the same area (Li et. al., 2023), which also  
421 reported higher emission fluxes of SQTs compared to other studies. This suggests that there  
422 may be a unique level of drought or plant characteristics that contribute to the high emission  
423 fluxes of SQTs in this region.

424

425 mechanism. The strong increase in SQT emission after irrigation in our study further  
426 supports the notion that enhanced synthesis of SQTs occurs shortly after the release of  
427 drought stress. In addition, the SQTs composition, like MTs composition, was observed to  
428 be more diverse after irrigation in most cases, warranting further study.

429



430 **Figure. 5** Diurnal SQT emission fluxes from the sampled branches. Column colors represent the emission  
 431 fluxes of four types of SQTs, and the magenta section of the columns refers to other SQTs. Yellow and blue  
 432 shading indicate the days before and after irrigation, respectively (see Sect. 2.4.2). Horizontal solid and  
 433 dashed lines are daytime mean and median SQT flux rates, respectively. AET values (see Sect. 2.4.4) are  
 434 marked in red and blue when they are larger than 1 or negative, respectively. To better present the trend on  
 435 26 Oct, a smaller figure with a smaller scale is added.

436  
 437 Interestingly, the high SQT emission rates found in this study are consistent with  
 438 the findings of a previous study conducted in the same area (Li et. al., 2023), which also  
 439 reported higher emission fluxes of SQTs compared to other studies. This suggests that there  
 440 may be a unique level of drought or plant characteristics that contribute to the high emission



441 fluxes of SQTs in this region. Furthermore, we found that the increase in SQT emission  
442 flux following irrigation (by 545% on average) was more significant than that of the MTs  
443 (by 150% on average). This suggests that the response of SQT emissions to water  
444 availability is stronger than that of MTs, which could be related to the chemical properties  
445 and physiological functions of SQTs in plants. Bonn et al. (2019) found that a sharp  
446 increase in SQT emission occurs close to the wilting point to protect the plant against  
447 oxidative damage, as also supported by Caser et al. (2019). The latter found that drought  
448 can induce the SQT synthesis mechanism. The strong increase in SQT emission after  
449 irrigation in our study further supports the notion that enhanced synthesis of SQTs occurs  
450 shortly after the release of drought stress. In addition, the SQTs composition, like MTs  
451 composition, was observed to be more diverse after irrigation in most cases, warranting  
452 further study.

453 Interestingly, the high SQT emission rates found in this study are consistent with  
454 the findings of a previous study conducted in the same area (Li et. al., 2023), which also  
455 reported higher emission fluxes of SQTs compared to other studies. This suggests that there  
456 may be a unique level of drought or plant characteristics that contribute to the high emission  
457 fluxes of SQTs in this region.

458  
459  
460  
461 ***3.3 The impact of meteorological parameters on MT and SQT emission rates under***  
462 ***drought condition***

463 The effect of meteorological conditions on BVOC emission rate under drought conditions  
464 is complex and depends on many factors, including vegetation type, BVOC type, and  
465 ambient stress. In the Eastern Mediterranean region, Li et al. (2023) found that under  
466 drought, the best proxy for BVOC emission is the instantaneous temporal change in RH;  
467 temporal changes in T were also better correlated with BVOC mixing ratio than absolute  
468 values of T. Here, we examined the impact of instantaneous changes in ambient air RH and  
469  $T - \delta_{RH}$  and  $\delta_T$ , respectively (see Sect. 2.4.3), as well as of ambient air T and RH on the  
470 BVOC emission rate. Due to the large variation in BVOC emissions across different  
471 branches, the r values were calculated separately for each branch and each sampling day.  
472 Figure 6 presents a principal component analysis (PCA) for the correlation of both  $\delta_{RH}$  and  
473  $\delta_T$  with the BVOC emission rates. Before irrigation, when the plants were under drought,  
474 on 8 Sep, 22 Sep, 19 Oct, and 26 Oct, the emission rates of ~~the both MTs and~~  
475 SQTs measured BVOC (including both MTs and SQTs) were better correlated with  $\delta_{RH}$   
476 and  $\delta_T$  (average Pearson's value (r) of 0.56 and -0.61, respectively) than with RH and T (r  
477 of -0.22 and 0.29, respectively). Exceptional are 14 Sep and 12 Oct, also sampled under  
478 drought conditions: on 14 Sep, the SQT emissions showed the best correlation with RH (r  
479 = 0.97); on 12 Oct, the emission rates of BVOCs tended not to correlate with any of the  
480 tested meteorological parameters because of a strong correlation of T and  $\delta_{RH}$  (r = -0.98).

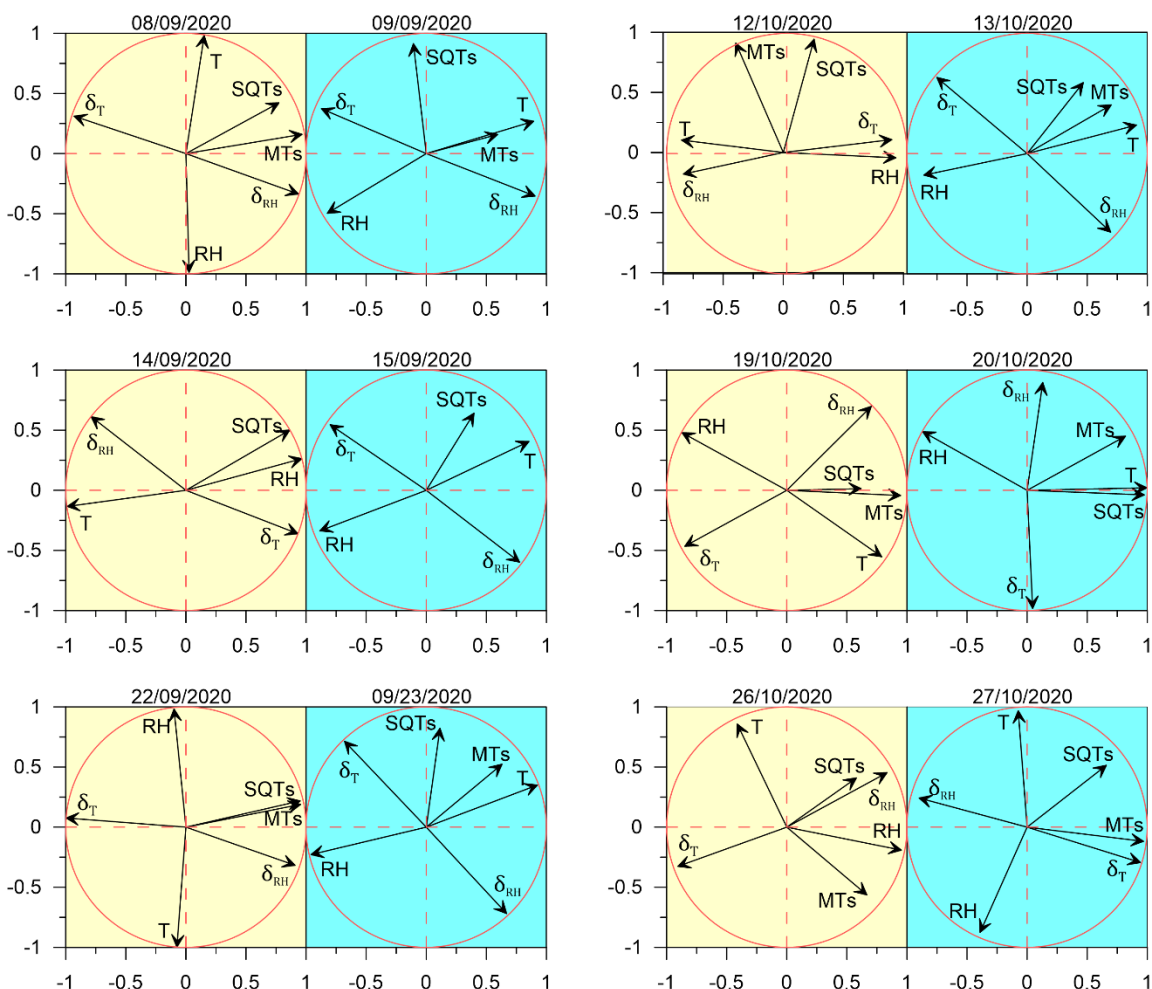
481 When focusing only on the days after irrigation, except for 27 Oct, the BVOC  
482 emissions were better correlated with T (~~on average averaging r values across all relevant~~  
483 days, r = 0.52) than with any other parameter. Interestingly, on 27 Oct, the SQTs tended to  
484 correlate with RH (-0.58), while the MT emission was better correlated with  $\delta_T$  (0.94). The  
485 PCA results show some similarities between the different sampled branches, in their

486 stronger response to  $\delta_{RH}$  than to the other tested meteorological parameters and their  
487 almost complete lack of correlation with T when under drought conditions. However, after  
488 irrigation, all BVOC emission rates were highly responsive to T, more than to any other  
489 parameter, reflecting the well-known Arrhenius-type increase for BVOC emission with  
490 temperature, as mentioned in Sect. 1.

491 Table 1 summarizes the correlation coefficients between the emission rates of  
492 SQTs/MTs and RH, T,  $\delta_{RH}$ , and  $\delta_T$ , both before and after irrigation. Considering the  
493 significant variability in the emission rates of SQTs and MTs across different branches, the  
494 r values presented in the table are averages calculated from individual branch-level r values,  
495 separately before and after irrigation. Li et al. (2023) showed that under drought conditions,  
496 the temporal gradient of meteorological parameters in general was more strongly correlated  
497 with BVOC emission rates – not only for RH, but also for T and vapor-pressure deficit.  
498 Before irrigation, both SQT and MT emission rates were more strongly correlated with  $\delta_{RH}$   
499 and  $\delta_T$  than with RH and T. However, after irrigation, the r values for the correlations with  
500  $\delta_{RH}$  and  $\delta_T$  were dramatically weakened. Moreover, following irrigation, the correlations  
501 and  $\delta_T$  than with RH and T. However, after irrigation, the r values for the correlations with  
502  $\delta_{RH}$  and  $\delta_T$  were dramatically weakened. Moreover, following irrigation, the correlations  
503 with T and RH for both MTs and SQTs were notably stronger than before the irrigation.  
504 This indicates that under drought, the temporal gradients in T and RH have a stronger  
505 impact on BVOC emissions than the absolute value of T and RH, in agreement with  
506 findings by Li et al. (2023). Here, we demonstrate that even a relatively minor precipitation  
507 event leads to T becoming the dominant factor in the BVOC emission rate, as expected

508 under non-drought conditions. Interestingly, after irrigation, the highest r value for MTs  
 509 was with T, but for SQTs, it was with RH.

510



511 **Figure. 6** PCA analysis for the response of SQTs and MTs to meteorological parameters. The results are  
 512 presented for SQTs, MTs, T, RH,  $\delta_T$ , and  $\delta_{RH}$ , individually for each measurement day. The yellow and blue  
 513 shaded areas refer to the day before and after irrigation, respectively.

514

515

516 with T and RH for both MTs and SQTs were notably stronger than before the irrigation.

517 This indicates that under drought, the temporal gradients in T and RH have a stronger

518 impact on BVOC emissions than the absolute value of T and RH, in agreement with

519 findings by Li et al. (2023). Here, we demonstrate that even a relatively minor precipitation  
520 event leads to T becoming the dominant factor in the BVOC emission rate, as expected  
521 under non-drought conditions. Interestingly, after irrigation, the highest r value for MTs  
522 was with T, but for SQTs, it was with RH.

523  
524 ~~Table 1 summarizes the correlation coefficients between the emission rates of~~  
525 ~~SQTs/MTs and RH, T,  $\delta_{\text{RH}}$ , and  $\delta_{\text{T}}$ , both before and after irrigation. Considering the~~  
526 ~~significant variability in the emission rates of SQTs and MTs across different branches, the~~  
527 ~~r values presented in the table are averages calculated from individual branch-level r values,~~  
528 ~~separately before and after irrigation. Li et al. (2023) showed that under drought conditions,~~  
529 ~~the temporal gradient of meteorological parameters in general was more strongly correlated~~  
530 ~~with BVOC emission rates — not only for RH, but also for T and vapor pressure deficit.~~  
531 ~~Before irrigation, both SQT and MT emission rates were more strongly correlated with  $\delta_{\text{RH}}$~~   
532 ~~and  $\delta_{\text{T}}$  than with RH and T. However, after irrigation, the r values for the correlations with~~  
533  ~~$\delta_{\text{RH}}$  and  $\delta_{\text{T}}$  were dramatically weakened. Moreover, following irrigation, the correlations~~  
534 ~~with T and RH for both MTs and SQTs were notably stronger than before the irrigation.~~  
535 ~~This indicates that under drought, the temporal gradients in T and RH have a stronger~~  
536 ~~impact on BVOC emissions than the absolute value of T and RH, in agreement with~~  
537 ~~findings by Li et al. (2023). Here, we demonstrate that even a relatively minor precipitation~~  
538 ~~event leads to T becoming the dominant factor in the BVOC emission rate, as expected~~  
539 ~~under non-drought conditions. Interestingly, after irrigation, the highest r value for MTs~~  
540 ~~was with T, but for SQTs, it was with RH.~~

541

542 **Table 1.** Correlation between the emission rates of MTs and SQTs and the examined meteorological  
 543 parameters. Presented are the Pearson's  $r$  values for the correlation between MT/SQT emission rate and RH,  
 544 T,  $\delta_{RH}$ , and  $\delta_T$  (green shading for SQT emissions and lavender shading for MT emissions). The values are  
 545 the average of  $r$  values for across multiple individual branches. -Blue and red shading indicates positive and  
 546 negative correlation, respectively, and the darkness of the color indicates their values. The  $P$ -values for the  
 547 correlation are shown in brackets.

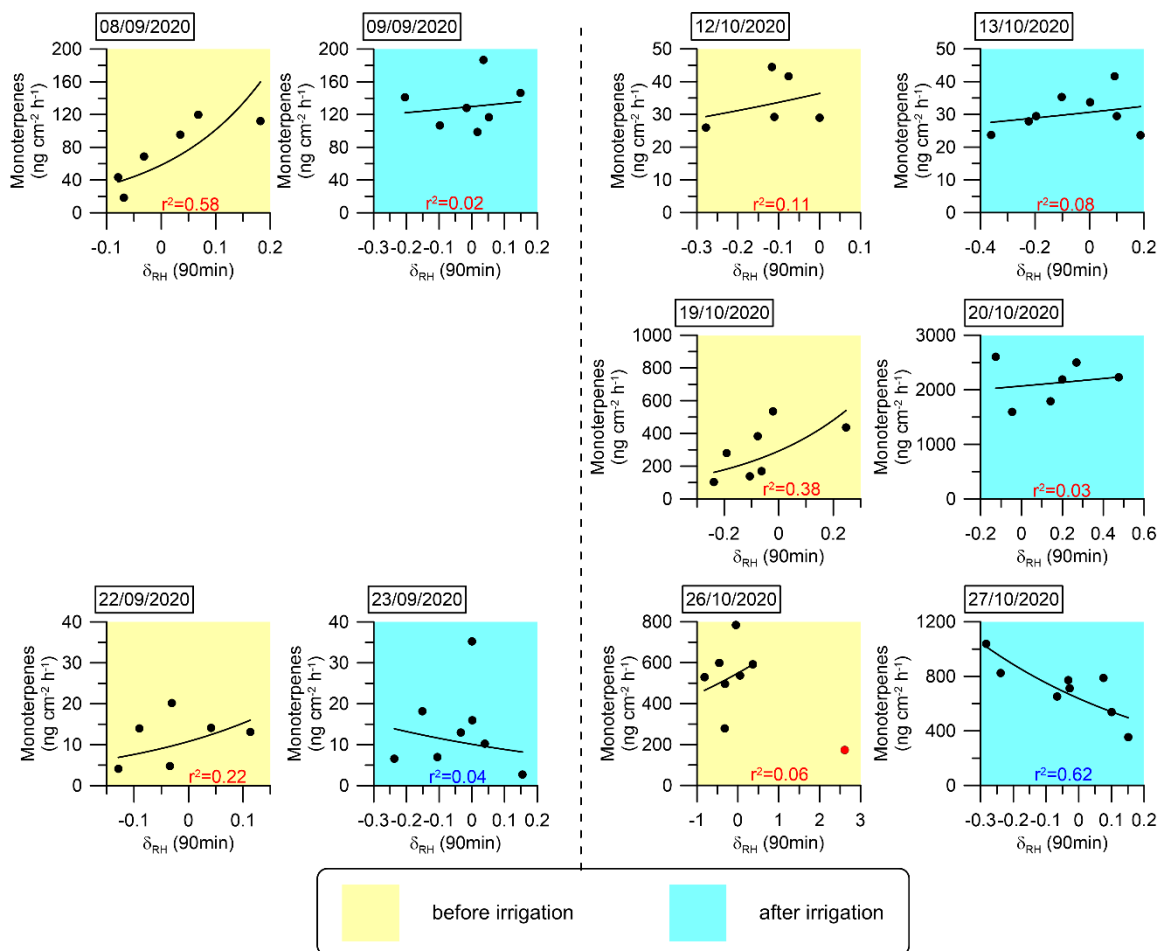
Pearson's $r$ value					
SQT	before irrigation	after irrigation	MT	before irrigation	after irrigation
vs RH	-0.22 (0.00)	-0.46 (0.00)	vs RH	-0.18 (0.11)	-0.44 (0.04)
vs T	0.33 (0.02)	0.42 (0.00)	vs T	0.20 (0.02)	0.46 (0.01)
vs $\delta_{RH}$	0.53 (0.02)	-0.11 (0.00)	vs $\delta_{RH}$	0.54 (0.01)	0.00 (0.00)
vs $\delta_T$	-0.50 (0.02)	0.13 (0.00)	vs $\delta_T$	-0.48 (0.01)	0.03 (0.00)

548  
 549 The analysis presented in Fig. 6 and Table 1 reinforces the finding that  
 550 instantaneous changes in meteorological parameters, particularly  $\delta_{RH}$ , serve as a better  
 551 proxy for BVOC emission rate under drought conditions. This finding suggests that  
 552 modeling BVOC emission rates under drought conditions can rely on  $\delta_{RH}$ . In light of this  
 553 insight, we investigated the mathematical connection between  $\delta_{RH}$  and the emission rates  
 554 of the MT and SQT fluxes. Exponential fitting corresponded with a relatively strong  
 555 correlation between these emission rates and  $\delta_{RH}$ . Other fitting types used to test this  
 556 relationship are presented in Sect. S2. Figures 7 and 8 depict the exponential fitting curves  
 557 for MTs and SQTs, respectively. These curves are presented separately for each branch  
 558 and individually for drought and post-irrigation conditions. The  $r^2$  for MTs with  $\delta_{RH}$  ranged  
 559 from 0.06 to 0.58 ( $r = 0.24$ – $0.76$ , average 0.48) under drought, whereas following irrigation,

560 the corresponding correlations ranged from 0.02 to 0.62 ( $r = -0.78$ – $0.28$ , average  $-0.08$ ).  
561 For SQTs, the corresponding  $r^2$  values were somewhat higher, ranging from 0.04 to 0.51 ( $r$   
562 =  $-0.41$ – $0.67$ , average  $+0.33$ ) and 0.00 to 0.48 ( $r = -0.69$ – $0.17$ , average  $-0.24$ ), under  
563 drought and following irrigation, respectively.

564 ~~Overall, these results suggest that while  $\delta_{RH}$  is likely a better proxy for MT and~~  
565 ~~SQT emission rates (see Table 1 and Sect. S3), the correlation of  $\delta_{RH}$  with these BVOCs~~  
566 ~~appears to be too weak to accurately predict their emission rates using  $\delta_{RH}$  values in~~  
567 ~~atmospheric modeling. Additional study is needed before  $\delta_{RH}$  can effectively serve as a~~  
568 ~~parameter for modeling BVOC emission rates.~~Following irrigation, the correlations  
569 between the emission flux rates and  $\delta_{RH}$  became more moderate (4 cases out of 11) or even  
570 negative (5 cases out of 11). This further demonstrates the high sensitivity of  $\delta_{RH}$ 's effect  
571 on BVOC emissions to changes in water availability. Further research is required to  
572 examine the physiological and biochemical processes underlying the sensitivity of BVOC  
573 emission rates to  $\delta_{RH}$ .

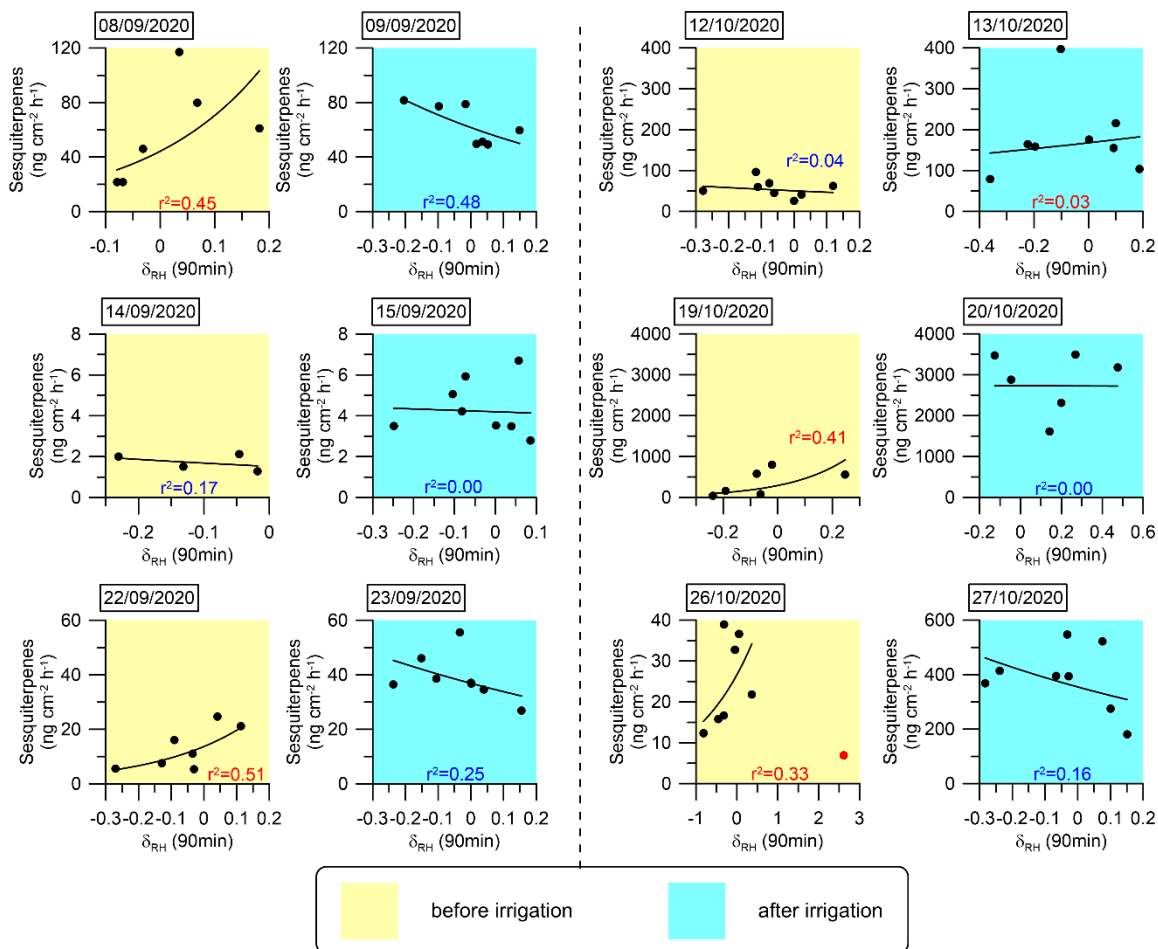
574



575 **Figure. 7** Daily correlations between MT emission fluxes and  $\delta_{RH}$ . An exponential fitting function was used  
 576 to fit the curves. The coefficient of determination ( $r^2$ ) for each day is marked in red or blue when the  
 577 correlation is positive or negative, respectively.

578 ~~Following irrigation, the correlations between the emission flux rates and  $\delta_{RH}$~~   
 579 ~~became more moderate (4 cases out of 11) or even negative (5 cases out of 11). This further~~  
 580 ~~demonstrates the high sensitivity of  $\delta_{RH}$ 's effect on BVOC emissions to changes in water~~  
 581 ~~availability. Further research is required to examine the physiological and biochemical~~  
 582 ~~processes underlying the sensitivity of BVOC emission rates to  $\delta_{RH}$ .~~





583

584 **Figure 8** Daily correlations between SQT emission fluxes and  $\delta_{RH}$ . An exponential fitting function was used  
 585 to fit the curves. The coefficient of determination ( $r^2$ ) for each day is marked in red or blue when the  
 586 correlation is positive or negative, respectively. The sample at 12:10 h on 26 Oct 2020 (marked in red) was  
 587 not considered in the fitting curve for that day, because an extremely sharp increase in RH (from 10 to 31%)  
 588 occurred within 10 min, which we considered an outlier.

589

590 Overall, these results suggest that while  $\delta_{RH}$  is likely a better proxy for MT and  
 591 SQT emission rates (see Table 1 and Sect. S3), the correlation of  $\delta_{RH}$  with these BVOCs  
 592 appears to be too weak to accurately predict their emission rates using  $\delta_{RH}$  values in  
 593 atmospheric modeling. Additional study is needed before  $\delta_{RH}$  can effectively serve as a  
 594 parameter for modeling BVOC emission rates.

595 Following irrigation, the correlations between the emission flux rates and  $\delta_{RH}$   
596 became more moderate (4 cases out of 11) or even negative (5 cases out of 11). This further  
597 demonstrates the high sensitivity of  $\delta_{RH}$ 's effect on BVOC emissions to changes in water  
598 availability. Further research is required to examine the physiological and biochemical  
599 processes underlying the sensitivity of BVOC emission rates to  $\delta_{RH}$ .

#### 602 **4 Summary and conclusions**

603 We investigated BVOC emission rates from branches of *Phillyrea latifolia* under both  
604 drought and minor irrigation conditions in the Eastern Mediterranean region, with the aim  
605 of assessing the influence of low precipitation levels and meteorological parameters on MT  
606 and SQT emission rates during drought stress. We found that leaf water content increases  
607 gradually under prolonged periods of drought, indicating the plant's enhanced capacity for  
608 water uptake under more severe drought conditions. The highest emission rate among all  
609 detected MTs was of *cis*- $\beta$ -ocimene, and among the detected SQTs,  $\beta$ -caryophyllene,  $\alpha$ -  
610 humulene, germacrene D, and  $\alpha$ -farnesene. Both the MT and SQT emission rates were  
611 significantly influenced by the availability of soil water. In response to irrigation, the MT  
612 and SQT emission rates increased by 150% and 545%, respectively, indicating that even a  
613 small amount of water (equivalent to 5.5–7 mm precipitation) can significantly impact their  
614 emission rates.

615 This study highlights the complex way in which meteorological conditions affect  
616 BVOC emissions under drought conditions. In line with Li et al.'s (2023) findings, under  
617 drought, the instantaneous change of relative humidity,  $\delta_{RH}$ , was the best proxy for BVOC  
618 emission rates, ~~considering the as its strong correlation between with~~ MTs and SQTs ~~and~~

619  $\delta_{RH}$  emission rate (r = 0.54 and 0.53, respectively) was the strongest among all tested  
620 meteorological parameters. However, after a small amount of irrigation (equivalent to 5.5–  
621 7 mm precipitation), no correlation was observed between  $\delta_{RH}$  and MT emission rate,  
622 whereas a negative correlation with  $\delta_{RH}$  was observed for SQT emission rate. The increase  
623 in soil water availability led to T (for MTs) or RH (for SQTs) becoming the dominant  
624 meteorological parameter affecting BVOC emission rate, making them the best proxies for  
625 BVOC emission rates among all tested meteorological parameters. This indicates that  
626 changes in water availability can dramatically alter the manner in which BVOC emissions  
627 respond to meteorological conditions.

628 Hence, according to the conditions used in this study, under more severe drought,  
629  $\delta_{RH}$  can serve as the best proxy for BVOC emission rate, whereas under more moderate  
630 drought, either T or RH is the best proxy for BVOCs, in agreement with previous findings  
631 presented in the companion paper by (Li et al., 2023). Our findings indicate that even a  
632 small amount of precipitation can lead to a transition from a drought to non-drought regime  
633 in terms of BVOC emission rates and the manner in which they respond to meteorological  
634 conditions.

635

636 **Author contribution.** ET designed the experiments, QL and GL carried out the field  
637 measurements, QL performed the data acquisition. QL performed the analytical analysis  
638 together with EB and EL. QL and ET led the data analyses with contributions from all co-  
639 authors. QL and ET prepared the manuscript with contributions from EB.

640

641 **Competing interests.** The authors declare that they have no conflict of interest.



643

## 644 **Acknowledgements**

645 This study was supported by the Israel Science Foundation, Grant Nos. 1787/15 and  
646 543/22. Eran Tas holds the Joseph H. and Belle R. Braun Senior Lectureship in Agriculture.

647

648

## 649 **References**

- 650 Asensio D., Peñuelas J., Llusà J., Ogaya R., Filella I., 2007. Interannual and interseasonal soil CO<sub>2</sub>  
651 efflux and VOC exchange rates in a Mediterranean holm oak forest in response to  
652 experimental drought. *Soil Biology and Biochemistry* 39(10),2471–2484.  
653 <https://doi.org/10.1016/j.soilbio.2007.04.019>.
- 654 Aydin Y.M., Yaman B., Koca H., Dasedemir O., Kara M., Altioek H., Dumanoglu Y., Bayram A., Tolunay  
655 D., Odabasi M., Elbir T., 2014. Biogenic volatile organic compound (BVOC) emissions from  
656 forested areas in Turkey: Determination of specific emission rates for thirty-one tree species.  
657 *The Science of the total environment* 490,239–253.  
658 <https://doi.org/10.1016/j.scitotenv.2014.04.132>.
- 659 Baldwin I.T., Halitschke R., Paschold A., Dahl C.C. von, Preston C.A., 2006. Volatile signaling in  
660 plant-plant interactions: "talking trees" in the genomics era. *Science (New York, N.Y.)*  
661 311(5762),812–815. <https://doi.org/10.1126/science.1118446>.
- 662 Berg A.R., Heald C.L., Huff Hartz K.E., Hallar A.G., Meddens A.J.H., Hicke J.A., Lamarque J.-F., Tilmes  
663 S., 2013. The impact of bark beetle infestations on monoterpene emissions and secondary  
664 organic aerosol formation in western North America. *Atmos. Chem. Phys.* 13(6),3149–3161.  
665 <https://doi.org/10.5194/acp-13-3149-2013>.
- 666 Blande J.D., Tiiva P., OKSANEN E., Holopainen J.K., 2007. Emission of herbivore-induced volatile  
667 terpenoids from two hybrid aspen (*Populus tremula* × *tremuloides*) clones under ambient and  
668 elevated ozone concentrations in the field. *Glob Change Biol* 13(12),2538–2550.  
669 <https://doi.org/10.1111/j.1365-2486.2007.01453.x>.
- 670 Bonn B., Magh R.-K., Rombach J., Kreuzwieser J., 2019. Biogenic isoprenoid emissions under  
671 drought stress: Different responses for isoprene and terpenes. *Biogeosciences* 16(23),4627–  
672 4645. <https://doi.org/10.5194/bg-16-4627-2019>.
- 673 Bracho-Nunez A., Knothe N.M., Welter S., Staudt M., Costa W.R., Liberato M.A.R., Piedade M.T.F.,  
674 Kesselmeier J., 2013. Leaf level emissions of volatile organic compounds (VOC) from some  
675 Amazonian and Mediterranean plants. *Biogeosciences* 10(9),5855–5873.  
676 <https://doi.org/10.5194/bg-10-5855-2013>.
- 677 Brillì F., Barta C., Fortunati A., Lerdau M., Loreto F., Centritto M., 2007. Response of isoprene  
678 emission and carbon metabolism to drought in white poplar (*Populus alba*) saplings. *New*  
679 *Phytol* 175(2),244–254. <https://doi.org/10.1111/j.1469-8137.2007.02094.x>.

680 Brillì F., Ciccioli P., Frattoni M., Prestininzi M., Spanedda A.F., Loreto F., 2009. Constitutive and  
681 herbivore-induced monoterpenes emitted by *Populus x euroamericana* leaves are key  
682 volatiles that orient *Chrysomela populi* beetles. *Plant, cell & environment* 32(5),542–552.  
683 <https://doi.org/10.1111/j.1365-3040.2009.01948.x>.

684 Cai M., An C., Guy C., 2021. A scientometric analysis and review of biogenic volatile organic  
685 compound emissions: Research hotspots, new frontiers, and environmental implications.  
686 *Renewable and Sustainable Energy Reviews* 149(13),111317.  
687 <https://doi.org/10.1016/j.rser.2021.111317>.

688 Calfapietra C., Fares S., Manes F., Morani A., Sgrigna G., Loreto F., 2013. Role of Biogenic Volatile  
689 Organic Compounds (BVOC) emitted by urban trees on ozone concentration in cities: A review.  
690 *Environmental pollution (Barking, Essex 1987)* 183,71–80.  
691 <https://doi.org/10.1016/j.envpol.2013.03.012>.

692 Caser M., Chitarra W., D'Angiolillo F., Perrone I., Demasi S., Lovisolo C., Pistelli L., Pistelli L., Scariot  
693 V., 2019. Drought stress adaptation modulates plant secondary metabolite production in  
694 *Salvia dolomitica* Codd. *Industrial Crops and Products* 129,85–96.  
695 <https://doi.org/10.1016/j.indcrop.2018.11.068>.

696 Curci G., Beekmann M., Vautard R., Smiattek G., Steinbrecher R., Theloke J., Friedrich R., 2009.  
697 Modelling study of the impact of isoprene and terpene biogenic emissions on European ozone  
698 levels. *Atmospheric Environment* 43(7),1444–1455.  
699 <https://doi.org/10.1016/j.atmosenv.2008.02.070>.

700 Dayan C., Fredj E., Misztal P.K., Gabay M., Guenther A.B., Tas E., 2020. Emission of biogenic volatile  
701 organic compounds from warm and oligotrophic seawater in the Eastern Mediterranean.  
702 *Atmos. Chem. Phys.* 20(21),12741–12759. <https://doi.org/10.5194/acp-20-12741-2020>.

703 Duhl T.R., Helmig D., Guenther A., 2008. Sesquiterpene emissions from vegetation: A review.  
704 *Biogeosciences* 5(3),761–777. <https://doi.org/10.5194/bg-5-761-2008>.

705 Filella I., Primante C., Llusà J., Martín González A.M., Seco R., Farré-Armengol G., Rodrigo A.,  
706 Bosch J., Peñuelas J., 2013. Floral advertisement scent in a changing plant-pollinators market.  
707 *Scientific reports* 3,3434. <https://doi.org/10.1038/srep03434>.

708 Fitzky A.C., Kaser L., Peron A., Karl T., Graus M., Tholen D., Halbwirth H., Trimmel H., Pesendorfer  
709 M., Rewald B., Sandén H., 2023. Same, same, but different: Drought and salinity affect BVOC  
710 emission rate and alter blend composition of urban trees. *Urban Forestry & Urban Greening*  
711 80(7),127842. <https://doi.org/10.1016/j.ufug.2023.127842>.

712 Fortunati A., Barta C., Brillì F., Centritto M., Zimmer I., Schnitzler J.-P., Loreto F., 2008. Isoprene  
713 emission is not temperature-dependent during and after severe drought-stress: A  
714 physiological and biochemical analysis. *The Plant journal for cell and molecular biology*  
715 55(4),687–697. <https://doi.org/10.1111/j.1365-313X.2008.03538.x>.

716 Genard-Zielinski A.-C., Boissard C., Fernandez C., Kalogridis C., Lathière J., Gros V., Bonnaire N.,  
717 Ormeño E., 2015. Variability of BVOC emissions from a Mediterranean mixed forest in  
718 southern France with a focus on *Quercus pubescens*. *Atmos. Chem. Phys.*  
719 15(1),431–446. <https://doi.org/10.5194/acp-15-431-2015>.

720 Genard-Zielinski A.-C., Boissard C., Ormeño E., Lathière J., Reiter I.M., Wortham H., Orts J.-P.,  
721 Temime-Roussel B., Guenet B., Bartsch S., Gauquelin T., Fernandez C., 2018. Seasonal

722 variations of *Quercus pubescens*; isoprene emissions from an *in*  
723 natura forest under drought stress and sensitivity to future climate change in the  
724 Mediterranean area. *Biogeosciences* 15(15),4711–4730. [https://doi.org/10.5194/bg-15-](https://doi.org/10.5194/bg-15-4711-2018)  
725 4711-2018.

726 Geron C., Daly R., Harley P., Rasmussen R., Seco R., Guenther A., Karl T., Gu L., 2016. Large  
727 drought-induced variations in oak leaf volatile organic compound emissions during PINOT  
728 NOIR 2012. *Chemosphere* 146,8–21. <https://doi.org/10.1016/j.chemosphere.2015.11.086>.

729 Giorgi F., Lionello P., 2008. Climate change projections for the Mediterranean region. *Global and*  
730 *Planetary Change* 63(2-3),90–104. <https://doi.org/10.1016/j.gloplacha.2007.09.005>.

731 Goldstein A.H., McKay M., Kurpius M.R., Schade G.W., Lee A., Holzinger R., Rasmussen R.A., 2004.  
732 Forest thinning experiment confirms ozone deposition to forest canopy is dominated by  
733 reaction with biogenic VOCs. *Geophys. Res. Lett.* 31(22),22,123.  
734 <https://doi.org/10.1029/2004GL021259>.

735 Greenberg J.P., Asensio D., Turnipseed A., Guenther A.B., Karl T., Gochis D., 2012. Contribution of  
736 leaf and needle litter to whole ecosystem BVOC fluxes. *Atmospheric Environment* 59,302–311.  
737 <https://doi.org/10.1016/j.atmosenv.2012.04.038>.

738 Guenther A., 2013. Biological and Chemical Diversity of Biogenic Volatile Organic Emissions into  
739 the Atmosphere. *ISRN Atmospheric Sciences* 2013(19),1–27.  
740 <https://doi.org/10.1155/2013/786290>.

741 Guenther A., Hewitt C.N., Erickson D., Fall R., Geron C., Graedel T., Harley P., Klinger L., Lerdau M.,  
742 McKay W.A., Pierce T., Scholes B., Steinbrecher R., Tallamraju R., Taylor J., Zimmerman P.,  
743 1995. A global model of natural volatile organic compound emissions. *J. Geophys. Res.*  
744 100(D5),8873–8892.

745 Guenther A.B., Jiang X., Heald C.L., Sakulyanontvittaya T., Duhl T., Emmons L.K., Wang X., 2012.  
746 The Model of Emissions of Gases and Aerosols from Nature version 2.1 (MEGAN2.1): An  
747 extended and updated framework for modeling biogenic emissions. *Geosci. Model Dev.*  
748 5(6),1471–1492. <https://doi.org/10.5194/gmd-5-1471-2012>.

749 Han Z., Zhang Y., Zhang H., Ge X., Gu D., Liu X., Bai J., Ma Z., Tan Y., Zhu F., Xia S., Du J., Tan Y., Shu  
750 X., Tang J., Sun Y., 2022. Impacts of Drought and Rehydration Cycles on Isoprene Emissions in  
751 *Populus nigra* Seedlings. *International journal of environmental research and public health*  
752 19(21). <https://doi.org/10.3390/ijerph192114528>.

753 Holopainen J.K., Gershenson J., 2010. Multiple stress factors and the emission of plant VOCs.  
754 *Trends in plant science* 15(3),176–184. <https://doi.org/10.1016/j.tplants.2010.01.006>.

755 Jiang X., Guenther A., Potosnak M., Geron C., Seco R., Karl T., Kim S., Gu L., Pallardy S., 2018.  
756 Isoprene Emission Response to Drought and the Impact on Global Atmospheric Chemistry.  
757 *Atmospheric environment (Oxford, England 1994)* 183,69–83.  
758 <https://doi.org/10.1016/j.atmosenv.2018.01.026>.

759 Kesselmeier J., Staudt M., 1999. Biogenic Volatile Organic Compounds (VOC): An Overview on  
760 Emission, Physiology and Ecology. *Journal of Atmospheric Chemistry* 33,23–88.

761 Li Q., Gabay M., Dayan C., Misztal P., Guenther A., Fredj E., Tas E., 2024. Instantaneous intraday  
762 changes in key meteorological parameters as a proxy for the mixing ratio of BVOCs over  
763 vegetation under drought conditions. *Atmos. Chem. Phys.*

764 Li Q., Gabay M., Rubin Y., Fredj E., Tas E., 2018. Measurement-based investigation of ozone  
765 deposition to vegetation under the effects of coastal and photochemical air pollution in the  
766 Eastern Mediterranean. *Science of The Total Environment* 645,1579–1597.  
767 <https://doi.org/10.1016/j.scitotenv.2018.07.037>.

768 Lionello P., 2012. *The Climate of the Mediterranean Region: From the Past to the Future*: Elsevier.

769 Llusia J., Roahtyn S., Yakir D., Rotenberg E., Seco R., Guenther A., Peñuelas J., 2016. Photosynthesis,  
770 stomatal conductance and terpene emission response to water availability in dry and mesic  
771 Mediterranean forests. *Trees* 30(3),749–759. <https://doi.org/10.1007/s00468-015-1317-x>.

772 Llusia J., Peñuelas J., 2000. Seasonal patterns of terpene content and emission from seven  
773 Mediterranean woody species in field conditions. *American J of Botany* 87(1),133–140.  
774 <https://doi.org/10.2307/2656691>.

775 Medrano H., Escalona J.M., Bota J., Gulías J., Flexas J., 2002. Regulation of photosynthesis of C3  
776 plants in response to progressive drought: Stomatal conductance as a reference parameter.  
777 *Annals of botany* 89 Spec No(7),895–905. <https://doi.org/10.1093/aob/mcf079>.

778 MIYASHITA K., TANAKAMARU S., MAITANI T., KIMURA K., 2005. Recovery responses of  
779 photosynthesis, transpiration, and stomatal conductance in kidney bean following drought  
780 stress. *Environmental and Experimental Botany* 53(2),205–214.  
781 <https://doi.org/10.1016/j.envexpbot.2004.03.015>.

782 Monson R.K., Jaeger C.H., Adams W.W., Driggers E.M., Silver G.M., Fall R., 1992. Relationships  
783 among Isoprene Emission Rate, Photosynthesis, and Isoprene Synthase Activity as Influenced  
784 by Temperature. *PLANT PHYSIOLOGY* 98(3),1175–1180.

785 Niinemets U., Loreto F., Reichstein M., 2004. Physiological and physicochemical controls on foliar  
786 volatile organic compound emissions. *Trends in plant science* 9(4),180–186.  
787 <https://doi.org/10.1016/j.tplants.2004.02.006>.

788 Niinemets U., Monson R.K., 2013. *Biology, controls and models of tree volatile organic compound*  
789 *emissions*. Dordrecht: Springer.

790 Nobel P.S., 1999. *Physicochemical & environmental plant physiology*. 2nd ed. San Diego:  
791 Academic Press.

792 Núñez L., Plaza J., Pérez-Pastor R., Pujadas M., Gimeno B.S., Bermejo V., García-Alonso S., 2002.  
793 High water vapour pressure deficit influence on *Quercus ilex* and *Pinus pinea* field  
794 monoterpene emission in the central Iberian Peninsula (Spain). *Atmospheric Environment*  
795 36(28),4441–4452. [https://doi.org/10.1016/S1352-2310\(02\)00415-6](https://doi.org/10.1016/S1352-2310(02)00415-6).

796 Owen S., Boissard C., Street R.A., Duckham S.C., Csiky O., Hewitt C.N., 1997. Screening of 18  
797 Mediterranean plant species for volatile organic compound emissions. *Atmospheric*  
798 *Environment* 31,101–117. [https://doi.org/10.1016/S1352-2310\(97\)00078-2](https://doi.org/10.1016/S1352-2310(97)00078-2).

799 Owen S.M., Hewitt C.N., 2000. Extrapolating branch enclosure measurements to estimates of  
800 regional scale biogenic VOC fluxes in the northwestern Mediterranean basin. *J. Geophys. Res.*  
801 105(D9),11573–11583. <https://doi.org/10.1029/1999JD901154>.

802 Pegoraro E., REY A.N.A., Abrell L., van HAREN J., LIN G., 2006. Drought effect on isoprene  
803 production and consumption in Biosphere 2 tropical rainforest. *Glob Change Biol* 12(3),456–  
804 469. <https://doi.org/10.1111/j.1365-2486.2006.01112.x>.



805 Peñuelas J., Munné-Bosch S., 2005. Isoprenoids: An evolutionary pool for photoprotection. Trends  
806 in plant science 10(4),166–169. <https://doi.org/10.1016/j.tplants.2005.02.005>.

807 Peñuelas J., Rutishauser T., Filella I., 2009. Ecology. Phenology feedbacks on climate change.  
808 Science (New York, N.Y.) 324(5929),887–888. <https://doi.org/10.1126/science.1173004>.

809 Peñuelas J., Staudt M., 2010. BVOCs and global change. Trends in plant science 15(3),133–144.  
810 <https://doi.org/10.1016/j.tplants.2009.12.005>.

811 Potosnak M.J., LeStourgeon L., Pallardy S.G., Hosman K.P., Gu L., Karl T., Geron C., Guenther A.B.,  
812 2014. Observed and modeled ecosystem isoprene fluxes from an oak-dominated temperate  
813 forest and the influence of drought stress. Atmospheric Environment 48,314–322.  
814 <https://doi.org/10.1016/j.atmosenv.2013.11.055>.

815 Ryan A.C., Hewitt C.N., Possell M., Vickers C.E., Purnell A., Mullineaux P.M., Davies W.J., Dodd I.C.,  
816 2014. Isoprene emission protects photosynthesis but reduces plant productivity during  
817 drought in transgenic tobacco (*Nicotiana tabacum*) plants. New Phytol 201(1),205–216.  
818 <https://doi.org/10.1111/nph.12477>.

819 Saunders S.M., Jenkin M.E., Derwent R.G., Pilling M.J., 2003. Protocol for the development of the  
820 Master Chemical Mechanism, MCM v3 (Part A): tropospheric degradation of non-aromatic  
821 volatile organic compounds. Atmos. Chem. Phys. 3,161–180.

822 Saunier A., Ormeño E., Boissard C., Wortham H., Temime-Roussel B., Lecareux C., Armengaud A.,  
823 Fernandez C., 2017. Effect of mid-term drought on *Quercus pubescens*  
824 BVOCs' emission seasonality and their dependency on light and/or temperature. Atmos. Chem.  
825 Phys. 17(12),7555–7566. <https://doi.org/10.5194/acp-17-7555-2017>.

826 Schade G.W., Goldstein A.H., Lamanna M.S., 1999. Are monoterpene emissions influenced by  
827 humidity? Geophys. Res. Lett. 26(14),2187–2190.

828 Seco R., Karl T., Turnipseed A., Greenberg J., Guenther A., Llusia J., Peñuelas J., Dicken U.,  
829 Rotenberg E., Kim S., Yakir D., 2017. Springtime ecosystem-scale monoterpene fluxes from  
830 Mediterranean pine forests across a precipitation gradient. Agricultural and Forest  
831 Meteorology 237-238,150–159. <https://doi.org/10.1016/j.agrformet.2017.02.007>.

832 Sindelarova K., Granier C., Bouarar I., Guenther A., Tilmes S., Stavrou T., Müller J.-F., Kuhn U.,  
833 Stefani P., Knorr W., 2014. Global data set of biogenic VOC emissions calculated by the MEGAN  
834 model over the last 30 years. Atmos. Chem. Phys. 14(17),9317–9341.  
835 <https://doi.org/10.5194/acp-14-9317-2014>.

836 Staudt M., Mandl N., Joffre R., Rambal S., 2001. Intraspecific variability of monoterpene  
837 composition emitted by *Quercus ilex* leaves. Can. J. For. Res. 31(1),174–180.  
838 <https://doi.org/10.1139/x00-153>.

839 Street R.A., Owen S., Duckham S.C., Boissard C., Hewitt C.N., 1997. Effect of habitat and age on  
840 variations in volatile organic compound (VOC) emissions from *Quercus ilex* and *Pinus pinea*.  
841 Atmospheric Environment 31,89–100. [https://doi.org/10.1016/S1352-2310\(97\)00077-0](https://doi.org/10.1016/S1352-2310(97)00077-0).

842 Tingey D., Turner D., Weber J., 1990. Factors Controlling the Emissions of Monoterpenes and  
843 Other Volatile Organic Compounds: U.S. Environmental Protection Agency, Washington, D.C.  
844 EPA/600/D-90/195 (NTIS PB91136622).

|845 Vilagrosa A., Bellot J., Vallejo V.R., Gil-Pelegrin E., 2003. Cavitation, stomatal conductance, and  
846 leaf dieback in seedlings of two co-occurring Mediterranean shrubs during an intense drought.  
847 Journal of experimental botany 54(390),2015–2024. <https://doi.org/10.1093/jxb/erg221>.  
|848